

# Effect of Polymer on Structural Characteristics and Steel Corrosion of Cement-Poor Mortar

I. JANOTKA and Ľ. KRAJČI

*Institute of Construction and Architecture, Slovak Academy of Sciences, SK-845 03 Bratislava  
e-mail: Ivan.Janotka@savba.sk*

Received 29 January 2003

Results of the study of styrene—acrylate dispersion influence on mechanical properties, hydrate phase, and pore structure formation as well as steel corrosion development in Portland cement mortar are discussed. Mortars with low cement content are used for the tests instead of usually studied mortars of cement-rich content. The object of interest was to ascertain the effect of polymer addition on cement-poor mortar behaviour using unfavourable mortar mixture composition and bad conditions for cement hydration. The specimens were exposed to 240-day dry (60 % R.H.) and wet (95 % R.H.) air cure at 20 °C. Polymer increases absorption capacity, capillarity, total pore volume, and porosity of the mortar relative to that without styrene—acrylate dispersion. Dynamic modulus of elasticity and compressive strength are declined. The main reason of this lies in lower bulky mass of hydrate phase and higher cumulative volume of pores in polymer-modified cement mortar (PMCM) compared to those found in control cement mortar (CCM). Air voids occur in PMCM instead of bulky cementitious material due to foaming effect of polymer. Its addition decreases alkalinity of cement mortar and increases the permeability, making the pore structure coarser than that formed in CCM. The capability of moist air transport through the bulk of mortars determines the corrosion rate of steel. Steel corrosion characteristics are evaluated by three independent methods indicating a close connection between the developed pore structure and the corrosion rate of steel in the mortars.

Polymer-modified mortars have been popular constructional materials for many years. Polymer dispersion can be diluted to various extents with mixing water. The demands placed on polymer dispersions for addition to cementitious binders are as follows [1]: *a)* the setting properties of the cement ought not to be impaired, *b)* the polymer ought not to be hydrolyzed by high alkalinity of the cement, and *c)* the polymer ought not to manifest considerable corrosive-promoting or strength-reducing effect on cement-based material. A wide range of research and development concerning cement—polymer composites has been done in the world already. Standardization work on the testing methods and quality requirements of cement—polymer composites has been in progress mainly in the United States, Japan, and the United Kingdom [2].

The important factors affecting the properties of polymer-modified mortars based on styrene-like dispersions polymerized with various monomer ratios are the variations of the polymer film strength, polymer film formability, and pore size distribution with changing bound styrene content and polymer to cement ratio [3]. Only when the above requirements have been satisfied, the various possible advantages to be gained from the use of polymer dispersions may be put for-

ward. In general, polymer-modified mortars have excellent resistance to atmospheric corrosion. The use of the polymer-modified mortars as repairing and finishing materials can be recommended in order to inhibit the corrosion of reinforcing steel bars in cement-rich and dense concrete structures [4]. From the adhesion mechanism of polymer modifiers to reinforcing steel bars it is clear that the bond between the polymer-modified mortar and reinforcing steel is the result of the presence of electrochemically active polymer cement co-matrixes at the interfaces, which helps to relax stresses during loading and retards the friction-controlled slip of the reinforcing steel bars [5].

The principle of polymer dispersions influence on cement-rich mortar and concrete according to the three-step simplified model of the structure formation was explained by *Afridi* [6]. The mixture of unhydrated cement particles and cement gel, on which polymer particles deposit partially, is typical for the first step. The second one is characterized by the mixture of cement gel and unhydrated cement particles enveloped with a close packed layer of polymer particles. Finally, the cement hydrates are enveloped with polymer films and membranes. The addition of polymers reduces the  $\text{Ca}(\text{OH})_2$  formation. The magnitude of reduction in quantity of  $\text{Ca}(\text{OH})_2$  is affected by the

polymer type. Polymer particles which adhere to the surface of  $\text{Ca}(\text{OH})_2$  crystals act as a kind of bond among  $\text{Ca}(\text{OH})_2$  particles and then precipitate in a special microstructure. Polymer particles filling in interstices on the contact zone reduce the space for the precipitation of  $\text{Ca}(\text{OH})_2$  [7]. This is the main reason of the reduced  $\text{Ca}(\text{OH})_2$  formation. The  $\text{Ca}(\text{OH})_2$  crystals are built up by the individual layers or plates which are joint together in a parallel fashion. The hydration products are very tightly situated around the layers or plates of the  $\text{Ca}(\text{OH})_2$  crystals. Such hydration products exert pressure with the increased age of hydration on  $\text{Ca}(\text{OH})_2$  layers or plates thereby pushing them together and making the  $\text{Ca}(\text{OH})_2$  crystals jointed to form a stack of them [8, 9]. By contrast with it, bad conditions for hydration in the mortar with polymer addition and the lack of cement contribute to the formation of the cement matrix rich in large pores and air voids. This results in high crystallization ability of the formed  $\text{Ca}(\text{OH})_2$  that proves in the final effect the increase in  $\text{Ca}(\text{OH})_2$ . It is suggested that polymer sets around the  $\text{Ca}(\text{OH})_2$  crystals and thus reinforces the contact between the surface of  $\text{Ca}(\text{OH})_2$  crystal and polymer. A portion of  $\text{Ca}(\text{OH})_2$  is adsorbed on the surface of polymer drops. The result of this interaction is mainly rosette-type arrangement of  $\text{Ca}(\text{OH})_2$  morphology in cement systems with polymer/cement ratio of 5 mass %. The atypical sheaf-like grains, or particles of this habit with sharp prickles on both the ends of the twin are suggested as to be the next modification of morphological type of  $\text{Ca}(\text{OH})_2$  crystal arisen on the polymer— $\text{Ca}(\text{OH})_2$  interfacial zone. It is believed that different spatial factor at the cement hydration and  $\text{Ca}(\text{OH})_2$  development in cement-rich and cement-poor mortar influences final amounts of the formed reaction products [10, 11].

A close relationship between pore structure and strength of cement composite is considered to be an integral consequence of the overall compositions and technological measures taken during its production as well as the process of development of the hydration products, upon which the composite strength depends. The pore structure is characterized by both the total volume of pores and relative representation of individual pores of various size, shape, and spatial arrangement [12]. The finer pore occurrence contributes to an increase in the interconnectivity of the pores. A migrating ionic species within a finer pore matrix has to traverse an unfractuous path to penetrate a small part of the matrix, whereas, if the pores are large, the migrating species may penetrate with alacrity. Transport of moist air in cement composites is carried out according to Fick's law. The capability of moist air to transport through the pore system in bulk of mortar may therefore determine the corrosion rate of embedded steel [13, 14]. The state of steel reinforcement is one of the most important utility properties of cement

composites. The related measurements are performed by suitable methods and techniques [15–17] indicating the corrosion of steel.

The present article is concerned with the study of structural characteristics and steel corrosion of the cement-poor mortar modified by styrene—acrylate dispersion. To examine in further details the dependence between strength, porosity, and corrosion of steel, the results of the tests are described.

## EXPERIMENTAL

Portland cement (CEM I 42.5 R, Holcim a.s., Rožhožník) [18] and standard sand specified by STN 72 1208 Standard [19] were used. Chemical composition and basic properties of the cement are listed in Table 1. Aqueous industrially made styrene—acrylate dispersion (Chemical Works CHZ Sokolov, Czech Republic) was applied as a cement modifier. Its main characteristics are reported in Table 2.

Mortar specimens at a mass ratio of cement to sand 1:5 and water to cement mass ratio ( $m_w/m_c$ ) of 0.5 were prepared [20]. The polymer to cement ratio was maintained at a constant level 5 mass % of cement,

**Table 1.** Composition and Properties of Portland Cement Employed

Component	$w_i/\text{mass } \%$
Insoluble residue	1.63
$\text{SiO}_2$	20.64
$\text{Al}_2\text{O}_3$	5.88
$\text{Fe}_2\text{O}_3$	3.13
$\text{CaO}$	61.49
$\text{MgO}$	1.34
$\text{SO}_3$	2.30
$\text{K}_2\text{O}$	1.82
$\text{Na}_2\text{O}$	0.53
Ignition loss	1.04
Major clinker phases according to Bogue	
	$w_i/\text{mass } \%$
$\text{C}_3\text{S}$	49.45
$\text{C}_2\text{S}$	21.88
$\text{C}_3\text{A}$	10.28
$\text{C}_4\text{AF}$	9.53
Density: $3\,140\text{ kg m}^{-3}$	
Surface area: $336.2\text{ m}^2\text{ kg}^{-1}$	
Initial set: 3 h 15 min	
Final set: 4 h 20 min	
3-Day cement strength: flexural 4.4 MPa	
compressive 23.5 MPa	
28-Day cement strength: flexural 7.9 MPa	
compressive 41.7 MPa	

Explanation of abbreviations in major clinker phases of the cement:  $\text{C}_3\text{S}$ :  $3\text{CaO} \cdot \text{SiO}_2$ ;  $\text{C}_2\text{S}$ :  $2\text{CaO} \cdot \text{SiO}_2$ ;  $\text{C}_3\text{A}$ :  $3\text{CaO} \cdot \text{Al}_2\text{O}_3$ ;  $\text{C}_4\text{AF}$ :  $4\text{CaO} \cdot \text{Al}_2\text{O}_3 \cdot \text{Fe}_2\text{O}_3$ .

**Table 2.** Basic Characteristics of Styrene—Acrylate Dispersion

Parameter	Values
$w(\text{Total solids})/\%$	48—52
pH at 20°C	8—10
Viscosity/(mPa s <sup>-1</sup> )	max. 200
Degree of hydrolysis in alkaline environment/%	max. 10
Median of particle size/(mm 10 <sup>-3</sup> )	0.1—0.3
Density/(g cm <sup>-3</sup> )	1.03
Surface tension/(mN m <sup>-1</sup> )	38—41

calculated on the basis of total solids in the dispersion. This polymer addition was recommended by the producer. Fresh mortars were compacted and moulded into 40 mm × 40 mm × 160 mm test prisms. The specimens were stored for 24 h at 20°C and 95 % R.H. – wet air. After demoulding one part was kept in a wet air for next 239 days, the second part was exposed to 20°C (60 % R.H.) – dry air cure for the same time.

The apparent density of mortars was estimated on mortar specimens of regular shape by weighting at the calculated volume of prisms. The density was ascertained by the pycnometric method. Total porosity (PS) was calculated in mass % from the measured apparent densities  $\rho_A$  and densities  $\rho$  using the formula

$$\text{PS} = (1 - \rho_A/\rho) \cdot 100 \quad (1)$$

where  $\rho_A$  is apparent density in kg m<sup>-3</sup> and  $\rho$  is density in kg m<sup>-3</sup>. Capillarity of water in the mortar specimens was estimated by the following way. The test specimens were stored in air with relative humidity of 100 % and temperature of 20°C during tests. The bottom of mortar prisms was immersed into water-saturated sand bed. Water was uptaken through the area of fresh broken piece of the specimen after flexural strength testing. The measured results were calculated in mass %. Compressive strength, dynamic modulus of elasticity, and absorption capacity of the mortars were determined according to standard procedures [20—22].

Powder X-ray diffraction patterns were recorded on Philips X-ray diffractometer coupled with an automatic data recording system. CuK $\alpha$  radiation was used. The thermograms were recorded on a Derivatograph Q 1 500. In general, 200 mg of each sample was heated at 20°C min<sup>-1</sup> from 20°C to 1 000°C. Pore structure study was performed using a high-pressure porosimeter mod. 2 000 and macroporosimetry unit mod. 120 (both Carlo Erba Science, Italy). From the results of mercury intrusion porosimetry (MIP) pore volume of micropores (to 7 500 nm) and macropores, median of micropore, and total pore radius as well as total porosity were estimated. This porosimetry unit enables measurements of pore radii between 3.75 nm and 0.2 mm.

Steel corrosion was tested by the method of electrode potential and method of electrical resistance [23] on steel reinforcement class 10 425 [24] embedded in prism specimens and on steel bars of the same class immersed into the water extracts of mortars using the potentiodynamic method [23].

The principle of the method of electrode potential lies in measurements of steel electrode potential (*vs.* saturated calomel electrode) in the currentless state as a characteristic of steel/mortar interface. Standard millivoltmeter MT 100 (Metra Blansko, Czech Republic) was used in the test. Method of electrical resistance with specially prepared steel corrosion sensor is based on the increase of its electrical resistance as a result of corrosion. Stabilized power supply (current source), transfer electrical unit, and millivoltmeter with sensitivity of 1  $\mu\text{V}$  are the essential equipment set for the experiment. Potentiodynamic method enables the gradual linear increasing of the steel potential. Simultaneously, the current flowing through three-electrode measuring system is recorded and electrochemical corrosion state is evaluated. Potentiodynamic curves of steel in mortar extract were obtained using Potentiostat OH-405 (Radelkis, Hungary) at a polarization rate of 30 mV min<sup>-1</sup>. The pH values of mortar extracts were determined by the pH-meter OP 113 (Radelkis, Hungary).

## RESULTS AND DISCUSSION

Usually the mortar of cement-rich content is investigated to describe its significant properties. On the contrary, we are interested in the cement-poor mortar with respect to its properties and the ability to protect steel against corrosion using unfavourable mortar mixture composition and bad conditions for cement hydration even with the polymer addition. This aspect would be regarded as an attempt of the other view of the research concerning cement—polymer interaction, and the influence of polymer on mortar properties.

The control cement mortar (CCM) and polymer-modified cement mortar (PMCM) exhibit lower compressive strength and dynamic modulus of elasticity relative to the mortars with a standard composition [20] (Table 3). This is due to a lack of bonding cement. The polymer addition increases markedly absorption capacity and total porosity of the mortar. Lower values of absorption capacity and total porosity indicate a finer pore structure in CCM relative to that formed in PMCM. This is clearly confirmed by specific surface area values. A lower specific surface area of PMCM shows a coarser character of developed pore structure with domination of large pores. A larger volume of finer pores contributes to higher specific surface area in CCM. This results in higher compressive strength and elasticity modulus values. Polymer addition lowers compressive strength and elasticity modulus of the mortars and enhances their permeability due to the

**Table 3.** Physicomechanical Properties and Total Porosity of Mortar Specimens

Property of the mortar	Curing*	Type of the mortar	
		CCM ( $m_w/m_c = 0.5$ )	PMCM ( $m_w/m_c = 0.5$ )
Density/( $\text{kg m}^{-3}$ )	W	2 574	2 629
Specific surface area/( $\text{m}^2 \text{kg}^{-1}$ )	W	449.9	302.5
Compressive strength/MPa	S	4.7	2.0
Elasticity modulus/GPa	W	8.1	2.9
Absorption capacity/mass %	S	10.0	2.1
Total porosity/mass %	W	16.1	4.2
	S	15.8	31.9
	W	15.3	25.6
	S	33.8	43.7
	W	31.0	41.8

\*S: 240-day (20 °C; 60 % R.H.) – dry air; W: 240-day (20 °C ; 95 % R.H.) – wet air.

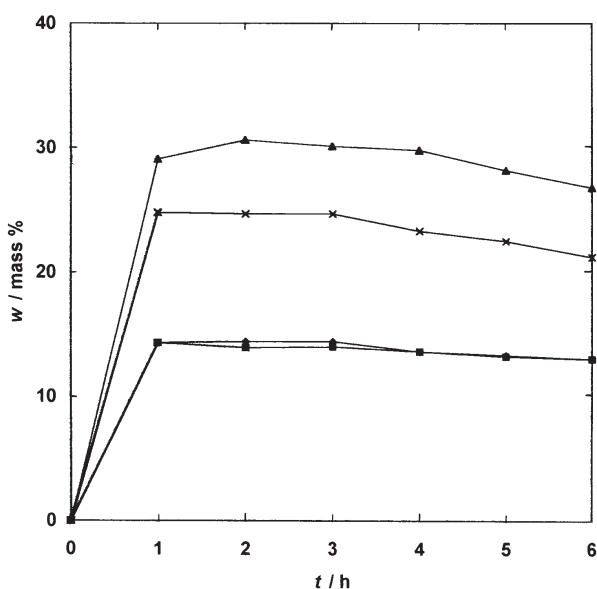


**Fig. 1.** Capillarity of water in mortar specimens exposed to 240-day dry air cure and wet air cure and then dried at 105 °C. Control cement mortar (CCM):  $\blacklozenge$  20 °C (60 % R.H.) – moist;  $\blacksquare$  20 °C (95 % R.H.) – moist, then dried at 105 °C. Polymer-modified cement mortar (PMCM):  $\blacktriangle$  20 °C (60 % R.H.) – moist;  $\times$  20 °C (95 % R.H.) – moist, then dried at 105 °C to the constant mass.

formation of coarser pore matrix. A higher total porosity of PMCM relative to CCM is the evident proof of this statement.

As expected, PMCM shows higher capillarity at both curing conditions relative to CCM (Fig. 1). This confirms a coarse character of developed pore structure in PMCM with a strong pore interconnectivity enabling easy water uptake. No difference between the capillarity of CCM cured either in wet or dry air is found. In contrast with it, the capillarity of PMCM kept in dry air is higher compared to that when the mortar is kept in wet air. This is caused by the different behaviour of polymer at heating to 105 °C. Cap-

illarity of dried PMCM is lower than that without desiccation at 105 °C. The temperature treatment of PMCM results in significantly strengthened interconnectivity of open pores in the mortar due to intense polymer bonds development in pore matrix at elevated temperatures.

The results of X-ray diffraction analysis (Fig. 2) show that the conversion of alite and belite to hydration products estimated by the reduction in intensity of diffraction patterns at 0.278 nm and 0.275 nm is higher in CCM than that in PMCM. The addition of polymer contributes to the increase in  $\text{Ca}(\text{OH})_2$  and decrease in  $\text{CaCO}_3$  contents in PMCM as a consequence of polymer addition. These interesting facts follow from the differential thermal analysis (DTA) study (Fig. 3). The results are evaluated by comparative study of the plots of DTA curves that gives a clear picture of tested materials behaviour. Polymer has an inert behaviour towards sand (curves 1 and 2). A bright exotherm between 315 °C and 350 °C in the polymer–sand system is the proof of dispersion decomposition (curve 2). The high intensity of the exotherm ranged between 315 °C and 350 °C in PMCM can be connected with the effect of mutual interaction of hydration products with polymer. A large endotherm between 100 °C and 300 °C on DTA curve of CCM (curve 3) proves the occurrence of gel-like hydration products, the sharp endotherm at 510 °C the dehydroxylation of  $\text{Ca}(\text{OH})_2$ , those at 560 °C  $\beta, \alpha\text{-SiO}_2$  modification and at 830 °C  $\text{CaCO}_3$  dissociation due to the  $\text{CO}_2$  release from  $\text{CaCO}_3$ . The endotherm between 100 °C and 300 °C on DTA curve belonging to PMCM (curve 4) is larger than that in CCM. This clearly confirms the superposition effect on the intensity of this endotherm by contemporary occurrence of gel-like hydration products and polymer in this temperature interval. However, the mutual interaction of hydration products with polymer has not been studied. The excess of sand in the mortars does not enable to do it. The  $\text{Ca}(\text{OH})_2$  content is slightly higher, and that of calcite is lower in PMCM relative to CCM.

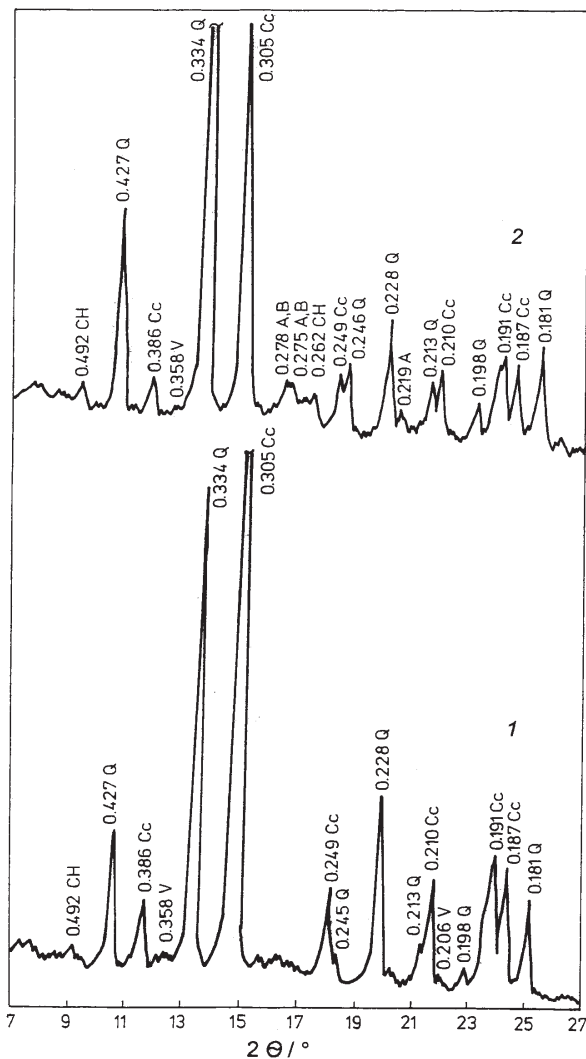


**Fig. 2.** X-Ray diffraction patterns of mortar specimens: 1. control cement mortar (CCM); 2. polymer-modified cement mortar (PMCM). CH – Ca(OH)<sub>2</sub>, Q – quartz SiO<sub>2</sub>, A – alite C<sub>3</sub>S, B – belite C<sub>2</sub>S, Cc – calcite CaCO<sub>3</sub>, V – vaterite CaCO<sub>3</sub>.

This gives evidence of polymer influence on the formed hydrate phase composition. It seems that the hydration products and Ca(OH)<sub>2</sub> formation are slightly promoted by polymer addition. The CCM is carbonated to a larger extent relative to PMCM. When polymer

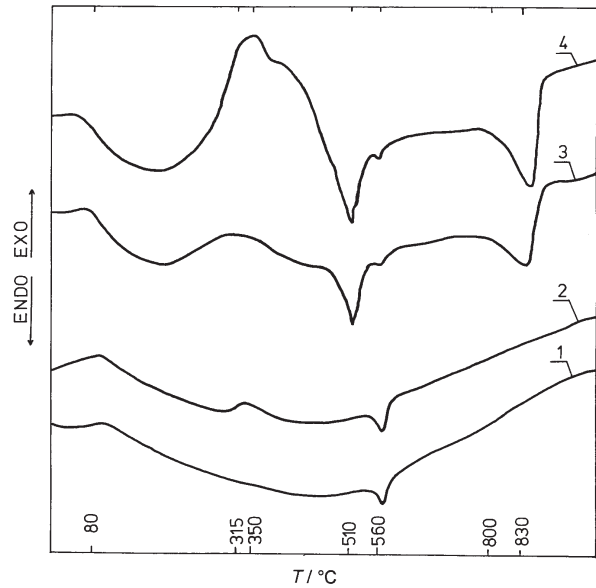


**Fig. 3.** DTA curves of sand and mortar specimens exposed to 240-day wet air cure: 1. sand; 2. sand with polymer as being 5 % of total solids in PMCM; 3. control cement mortar (CCM); 4. polymer-modified cement mortar (PMCM).

is added compressive strength and dynamic modulus of elasticity of the mortar are decreased, whereas absorption capacity, total porosity, and capillarity are increased. Polymer addition has a straight consequence on the hydrate phase and pore structure development. The lower bulky mass of hydrate phase, the coarser pore structure due to air voids occurrence. This results in the decreased compressive strength and elasticity modulus even at higher amount of the formed Ca(OH)<sub>2</sub> in PMCM compared to CCM.

The MIP results (Table 4) show significantly higher median of total pore radius and total porosity values in PMCM relative to CCM. This confirms the effect of pore structure coarsening due to polymer addition. CCM indicates the lower cumulative volume of pores at the same pore radius compared to that found in PMCM (Fig. 4). The pore structure of PMCM is coarser and therefore more permeable than that of CCM.

The pH value of CCM water extract is 11.93 and

**Table 4.** Pore Structure Study of Mortar Specimens

Type of mortar	N <sub>r</sub> (Micropores to 7 500 nm)/%	Median of		Total porosity %
		micropore radius	pore radius	
		nm	nm	
CCM	52.9	64.4	3 280	16.6
PMCM	49.2	89.4	7 215	27.3

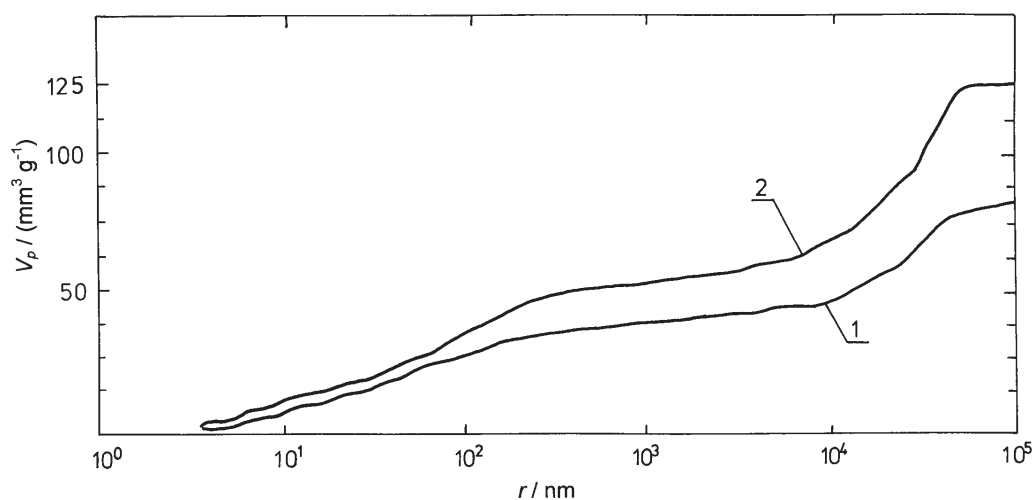


Fig. 4. The dependence of pore volume on pore radius: 1. control cement mortar (CCM); 2. polymer-modified cement mortar (PMCM), exposed to 240-day wet air cure.

Table 5. The pH Values of Water Extracts of Mortar Specimens

Type of mortar	Characterization of measured specimen	pH Value
CCM	Surface layer of the mortar	11.81
	Core layer of the mortar	12.05
	Average mortar sample	11.93
PMCM	Surface layer of the mortar	10.81
	Core layer of the mortar	11.41
	Average mortar sample	11.11

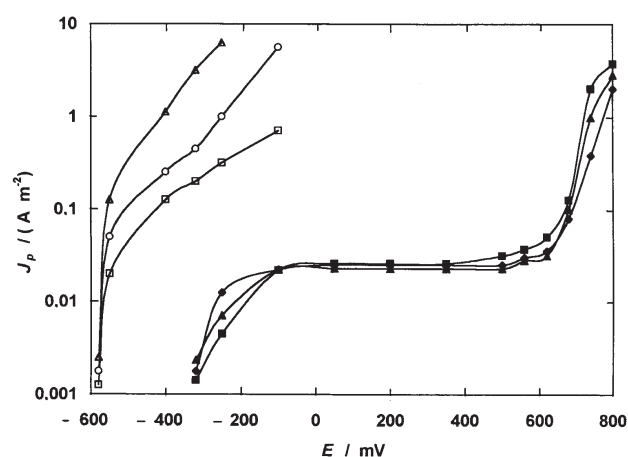


Fig. 5. Potentiodynamic curves of steel in water extracts of mortar specimens after 240-day wet air cure:  $\blacklozenge$  control cement mortar (CCM);  $\blacktriangle$  CCM – core layer,  $\blacksquare$  CCM – surface layer;  $\triangle$  polymer-modified cement mortar (PMCM);  $\circ$  PMCM – core layer,  $\square$  PMCM – surface layer.

that of PMCM water extract is 11.11 (Table 5). This slight decrease in pH is influenced by polymer addition. Alkalinity of cement-rich mortars is usually

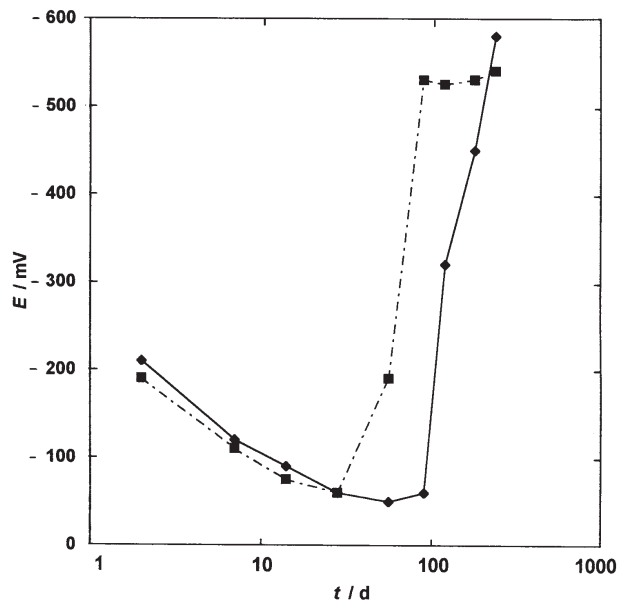


Fig. 6. Time dependence of changes in electrode potential of embedded steel reinforcement:  $\blacklozenge$  control cement mortar (CCM);  $\blacksquare$  polymer-modified cement mortar (PMCM), exposed to 240-day wet air cure.

about  $12.4 \pm 0.2$ . The lack of cement is the reason of lower pH values of mortar extracts. Potentiodynamic curves of steel (Fig. 5) in CCM water extracts show a distinct passive zone indicating the suitable conditions for steel passivation even at lower pH of 11.93. Passive zone represents the part of curve parallel with  $x$ -axis. Steel is active in PMCM water extracts (Fig. 5, Table 5). Steel is passive in CCM until 90-day exposure in wet air when measured by the method of electrode potential of steel (Fig. 6) and the method of electrical resistance of steel (Fig. 7). Passive state of steel is maintained in PMCM until 56-day exposure in wet air cure. The corrosion process is proved

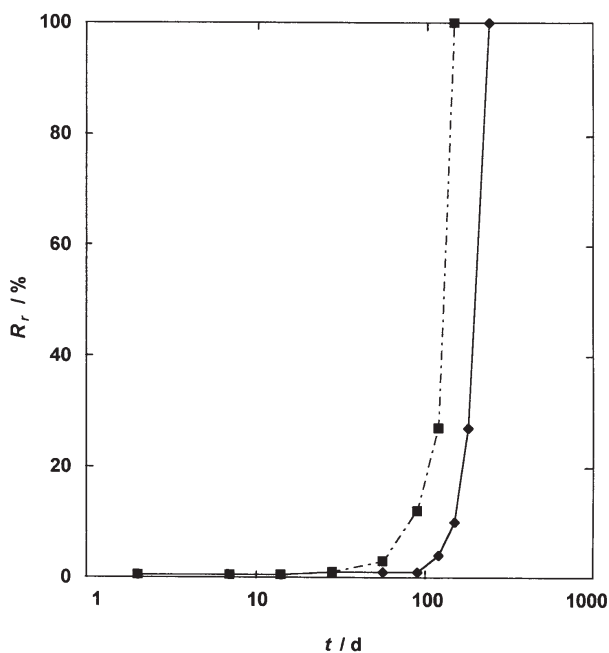


Fig. 7. Time dependence of the increase in electrical resistance of embedded steel reinforcement:  $\blacklozenge$  control cement mortar (CCM);  $\blacksquare$  polymer-modified cement mortar (PMCM), exposed to 240-day wet air cure.

by the significant decrease in electrode potential and the increase in electrical resistance of steel. Low passivation ability of both mortars is caused by the low cement content. The loss in passivity of steel is accelerated by polymer addition. However, an evident disproportion among the results of potentiodynamic method and methods of electrode potential and electrical resistance of steel in CCM was found. Steel is in electrochemically passive state according to the potentiodynamic method, whereas two other methods prove the active state of steel. Potentiodynamic method concerns only the straight influence of the mass of mortar including polymer addition on the electrochemical behaviour of steel. The developed pore matrix, the effect of pore size distribution and time upon which steel is exposed to wet air cure is not taken into account by the potentiodynamic method. Therefore this method is not suitable for steel corrosion measurement of cement-poor mortars. The measurements done by the method of electrode potential and the method of electrical resistance of steel are, on the contrary, time-dependent on moist air transport through the developed pore structure of tested mortars. The porosity parameters (total pore volume, pore size, pore median radius) of the mortar influence the corrosion rate of embedded steel. Polymer enhances the inclination of steel to corrosion mainly due to the coarser and more permeable pore matrix of the mortar for a moisture transport. The next important role is played by the decreased alkalinity of PMCM. The study of polymer influence on the pore structure development and cor-

rosion rate of steel is easily performed in cement-poor mortars. The influence of polymer on the developed pore structure and consequently on steel corrosion rate is eliminated in cement-rich mortars due to the higher cement content reducing markedly the danger of steel corrosion.

## CONCLUSION

Conversion of unhydrated  $C_3S$  and  $C_2S$  (see Table 1) to hydration products is slower in PMCM than that in CCM. Mutual interaction between hydration products and styrene-acrylate dispersion forming complex salts is possible but not proved in mortars rich in sand. Polymer addition promotes the  $Ca(OH)_2$  formation and retards carbonation of the mortar relative to the control one.

Polymer addition has a straight effect on the pore structure development. The coarse pore structure with extremely high pore median radius and total porosity is formed in PMCM. Consequently, the compressive strength and elasticity modulus are decreased when compared to CCM with a finer pore structure.

High absorption capacity and capillarity values of PMCM relative to those of CCM also indicate coarse and permeable pore matrix. This enables easy transport of moisture throughout the bulk of PMCM. The formed permeable pore matrix and decreased alkalinity of PMCM cause the accelerated loss in passivity of steel relative to CCM.

*Acknowledgements.* The authors wish to thank the Slovak Grant Agency VEGA (Grant No. 2/3036/23) for the support of this work.

## REFERENCES

1. Taichman, H., in *Polymer Dispersions for Cement and Concrete, 1st International Congress on Polymer Concretes*, June 4–6, Hannover, Germany, 1975. Communications p. 1, Session D, Paper 2.
2. Ohama, Y., *Adv. Cem. Chem. Bond. Ceram.* 13, 79 (1989).
3. Ohama, Y., Demura, K., Hamatsu, M., and Kakegava, M., *ACI Mater. J.* 88, 56 (1991).
4. Ohama, Y., Demura, K., and Kobayashi, K., *Cem. Concr. Res.* 21, 309 (1991).
5. Pareek, S. N., Ohama, Y., and Demura, K., *Trans. Jap. Concr. Inst.* 13, 567 (1991).
6. Afridi, M. V. K., Ohama, Y., Iqbal, M. Z., and Demura, K., *Int. J. Cem. Comp. Light. Concr.* 11, 235 (1989).
7. Chandra, S., Flodin, P., and Berntsson, L., in *Interaction between Calcium Hydroxide and Styrene-Methacrylate Polymer Dispersion, 3rd International Congress on Polymers in Concrete*, October 22–24, Koriyama, Japan, 1981, p. 125.
8. Afridi, M. V. K., Ohama, Y., Iqbal, M. Z., and Demura, K., *Cem. Concr. Res.* 20, 163 (1990).
9. Afridi, M. V. K., Ohama, Y., Demura, K., and Iqbal, M. Z., *Cem. Concr. Res.* 23, 484 (1993).

10. Janotka, I., Števula, L., and Frťalová, M. D., *Build. Res. J.* 42, 101 (1993).
11. Janotka, I., Madejová, J., Števula, L., and Frťalová, M. D., *Cem. Concr. Res.* 26, 727 (1996).
12. Jambor, J., *Stav. čas.* (in Slovak) 33, 743 (1985).
13. Kumar, A. and Roy, D. M., in *Pore Structure and Ionic Diffusion in Admixture Blended Cement Systems, 8th International Congress on the Chemistry of Cement*, May 2—5, Rio de Janeiro, Brazil, 1986. Communications 4, p. 73.
14. Bernaudat, F. and Revertegat, E., in *Modelisation of Transport Phenomena in Alternation Process of Cement Pastes, 8th International Congress on the Chemistry of Cement*, May 2—5, Rio de Janeiro, Brazil, 1986. Communications 4, p. 41.
15. Janotka, I., Krajči, L., Komloš, K., Frťalová, D., and Halás, P., *ACI Mater. J.* 89, 223 (1992).
16. Živica, V., Krajči, L., Bágel, L., and Vargová, M., *Constr. Build. Mater.* 11, 99 (1997).
17. Krajči, L., in *Reliability of Potentiodynamic Method in Monitoring of Steel Corrosion in Concrete, International Conference on Quality and Reliability in Building Industry*, October 27—29, Levoča, Slovakia, 1999, p. 265.
18. Slovak Technical Standard STN P ENV 197-1 Cement, Composition, Specification and Conformity Criteria – Part I: Common Cements (in Slovak).
19. Slovak Technical Standard STN 72 1208 Testing Sands (in Slovak).
20. European Technical Standard EN 196-1 Methods of Testing Cement – Part 1: Determination of Strength.
21. Slovak Technical Standard STN 73 1371 Method of Ultrasonic Pulse Testing of Concrete (in Slovak).
22. Slovak Technical Standard STN 72 2448 Testing of Moisture Content and Absorptivity of Mortar (in Slovak).
23. Slovak Technical Standard STN 73 1341 Corrosion Protection of Reinforcement Provided by Properties of Concrete. Methods of Test (in Slovak).
24. Slovak Technical Standard STN 41 0425 Steel 10 425 (in Slovak).